Int J Energy Environ Eng (2014) 5:279–290
DOI 10.1007/s40095-014-0138-9

ORIGINAL RESEARCH

Potential and properties of marine microalgae *Nannochloropsis oculata* as biomass fuel feedstock

Sukarni · Sudjito · Nurkholis Hamidi · Uun Yanuhar · I. N. G. Wardana

Received: 3 March 2014 / Accepted: 1 August 2014 / Published online: 29 August 2014

Abstract Microalgal biomass is the most promising and attractive alternative to replace the terrestrial crop utilization for renewable biomass fuel feedstock. The potential for biomass fuel is due to its fast growth rate and high ability for CO_2 fixation as compared to terrestrial vegetation. There are many species in the globe, growing both in marine and freshwater. In this work, the marine microalgae *Nannochloropsis oculata* (*N. oculata*) had been investigated in terms of potential abundance and physicochemical properties, which determine its feasibility as biomass fuel feedstock. The chemical composition was evaluated by energy-dispersive X-ray spectrometry, and the proximate analysis was done by performing experiments in the thermal gravimetric analyzer. During 7 days of cultivation, the average rate of increase in algal biomass was about 1.5×10^6 cells/ml/day. The proximate analysis of *N. oculata* indicated that it had compositions of low moisture content and fixed carbon, whereas high volatile matter and ash content, i.e., 3.99, 8.08, 67.45, and 24.47 %, respectively. The energy content, which was calculated through the proximate analysis results, was 16.80 MJ/kg. The algal biomass and its residue after 1,200 °C were characterized by Fourier transform infrared spectroscopy to investigate their chemical macromolecular compounds. This present study concludes that *N. oculata* is feasible as biomass fuel feedstock, either to direct or co-combustion mode by giving special attention to high ash content.

Keywords Renewable · Biofuel · Microalgae · *Nannochloropsis oculata* · Biomass fuel feedstock

Sukarni
Doctoral Program of Mechanical Engineering, Faculty of Engineering, University of Brawijaya, Malang, Indonesia

Sukarni (✉)
Department of Mechanical Engineering, Faculty of Engineering, State University of Malang, Malang, Indonesia
e-mail: sukarni.ft@um.ac.id

Sudjito · N. Hamidi · I. N. G. Wardana
Department of Mechanical Engineering, Faculty of Engineering, University of Brawijaya, Malang, Indonesia
e-mail: sudjitospn@yahoo.com

N. Hamidi
e-mail: nurkholishamidi@yahoo.com

I. N. G. Wardana
e-mail: wardana@ub.ac.id

U. Yanuhar
Biotechnology Laboratory, Department of Water Resources Management, Faculty of Fisheries and Marine Sciences, University of Brawijaya, Malang, Indonesia
e-mail: uunyanuhar@yahoo.com

Introduction

Since fossil fuel sources across the globe are fast depleting, renewable and non-conventional energy sources are urgent to explore to ensure the world is not threatened by a vacuum of energy. Biomass is generally defined as any hydrocarbon material, mainly consists of carbon, hydrogen, oxygen, and nitrogen [1]. It has been recognized as a major world renewable energy source to supplement declining fossil fuel resources [2]. However, the use of first-generation biofuels, which have been mostly taken from food and oil crops, such as rapeseed oil, sugar cane, sugar beet, maize, vegetable oils, and animal fats [3], has generated a lot of controversies, primarily because of their impact on global food markets and food security [4]. Hence, it drives the need to base non-food biomass resource biofuels. As a result, interests in aquatic biomass as the feasible fuel

source have recently gained prominence. One of the potential aquatic biomass for fuel is microalgae.

Microalgae will be potential as an important energy source in the future due to their potentially abundant, renewable, and CO_2 neutral fuel [5]. Compared with wood and land crops, microalgae are able to reproduce their biomass very rapidly and are very rich of oil content. Biomass productivity of microalgae can be 50 times more than that of the fastest growing terrestrial plant, namely switch grass [6]. Microalgae multiply their biomass about 1–3 per day [7] and theoretically can produce oil per hectare 100 times higher than that of terrestrial crops [8]. In the appropriate culture media, some algae can achieve very high lipid content, such as *Chlorella emersonii* [9], *Neochloris oleabundans* [10], and *Scenedesmus abundans* [11], which their lipid content up to 63, 56, and 67 %, by dry weight, respectively. Microalgae consume 2 g of CO_2 to produce 1 g of biomass when considering the glucose conversion into starch or lipids. Thus, by assuming a growth rate of 50 g/m^2/day, it is possible for one hectare pond algae to absorb up to one ton of CO_2 per day [12]. Thereby, microalgae cultures will neutralize CO_2 from their combustion.

Beyond the potential of microalgae for fuel in the future mentioned above, harnessing energy from microalgae must be considered in full transparence of physical and chemical properties. These properties are essential parameters for biomass fuel feedstock because they will affect both their combustion characteristics and proper handling modes in the furnace. The moisture content is very important property affecting the burning characteristics of biomass [13], mainly owing to its necessary of energy for releasing before a combustion process takes place. Hence, it will reduce the temperature in the combustion chamber. To ensure the sustained combustion process, this parameter must be exactly well known. Volatile matter content has also been indicated to affect the thermal behavior of solid fuels. The rate of volatile releases and its quantity determine the flame ignition, stability, and temperature profile in the radiation part of the furnace. Chemical properties of biomass are also a critical parameter as they determine the amount of energy contained in biomass. Likewise, the presence of the inorganic component in the biomass influence in the formation of ash, slag deposits, corrosion of boiler components, and aerosol [14]. Generally the inorganic constituents of biomass are Si, Ca, K, Na, Mg, S, P, Fe, Mn, and Al [15, 16], and the concentration of each element in biomass varies in accordance with the kind of species and growing environment. During combustion processes, part of the ash-forming compounds in the biomass mainly alkali metals and chlorine are volatilized into a gas phase, such as HCl(g), KCl(g), $(KCl)_2$(g), K_2SO_4(g), KOH(g), K(g), Na_2SO_4(g), and NaCl(g) [17, 18]. As cooling proceeds in the heat exchanger section of boilers, subsequent nucleation or condensation lead to the gases, together with solid phase submicron particles released from the fuel bed, form a large part of the fine ash particles. Otherwise, the compounds composed of Mg, Ca, Fe, Al, and non-metallic elements such as S, P, and Si are relatively more stable and less volatilized [19]. The fractions of non-volatilized compounds are remaining in the charcoal, and through a process of coalescence or melting form ash particles with a variety of shapes, sizes, and compositions, parallel to the characteristics of the parent material [20]. Therefore, to make biomass thermal conversion processes effective, these parameters must be clearly studied.

This work aimed to provide fundamental information for biomass fuel feedstock of *N. oculata* by investigating the biomass growth in the culture medium and its properties which affect the performance of biomass fuel including the calorific value, moisture content and physicochemical properties. The Fourier transform infrared (FTIR) spectroscopy analysis of both biomass and its residue were also conducted to identify the cellular macromolecular content.

The description of species

N. oculata is a species of a genus *Nannochloropsis*. It is a unicellular small green alga, found in both marine and freshwater [21, 22]. This alga is characterized by spherical or slightly ovoid cells [23] with a diameter of 2–5 μm [24] and absence of chlorophyll *b* and cellular xanthophyll pigment [25–27]. There is one chloroplast in each cell, without pyrenoid. Chloroplast endoplasmic reticulum is continuous with the nuclear envelope. Inside the chloroplast are lamellae, consisting of three thylakoids for each. Only one chlorophyll is present, namely chlorophyll *a* and the main pigment is violaxanthin. Its cell walls are composed of two components, the fibrillar component and the amorphous component. Fibrillar part forms the skeleton of the wall, which is embedded in the matrix of amorphous component. The most common fibrillar component is cellulose, a polymer of 1,4 linked β-D-glucose. An amorphous mucilaginous material is arranged from proteins, lipids, and polysaccharides. Occasionally, silica, calcium carbonate, or sporopollenin is also present as encrusting substances [28].

Nannochloropsis is widely distributed in oceans worldwide. It plays significant roles in the global carbon and mineral cycles [29]. This microalgae contains rich proteins, pigments, and polyunsaturated fatty acids [26, 30, 31], and it is commonly used in aquaculture as feed [32, 33]. In recent years, *Nannochloropsis* has been proposed as an excellent candidate for biofuel production [34, 35].

Methods

Microorganism and culture conditions

The *N. oculata* strain was obtained from the Institute of Brackish Water Aquaculture (BBAP) Situbondo, East Java, Indonesia. This species was cultured in an open pond with seawater medium in which its salinity and pH were 34 ‰ and 8.6, respectively. The culture medium was enriched with fertilizers whose composition was presented in Table 1. The use of fertilizers was 1 ml/l of the cultivation medium. The cultivation had been performed for 7 days.

Growth evaluation

The biomass productivity of *N. oculata* was evaluated daily by means of counting the number of cells in the culture medium using hemocytometer and optical microscope (CH2 Olympus optical Co. Ltd, Tokyo, Japan). Measurement was carried out every day at 11:00 AM during the cultivation period. Each measurement was repeated 3 times and the results were averaged.

The *N. oculata* specific growth rate, which was the change of the natural log of the cell number density (C_n) with time (t), was calculated from the slope of the linear regression of time (days) and cell density (cells/ml) [36]:

$$\mu = \mathrm{d}\ln C_n/\mathrm{d}t = (\ln C_t - \ln C_o)/(t - t_o) \quad (1)$$

where C_t is cell density at time (t), and C_o is cell density at the start of the exponential phase (t_o).

The time required to double the cell of *N. oculata*, termed the doubling time (day), could be estimated by equation:

$$t_d = \ln 2/\mu \quad (2)$$

Harvesting and drying

The biomass was harvested by precipitating it with caustic soda (NaOH); then it was filtered and washed twice with distilled water. Subsequently, the biomass sediment was dried in an oven at 80 °C for 24 h. The dried microalgae chunks were pulverized by the mortar to be fine particles and then finally stored in desiccators.

Table 1 The composition of fertilizers used for culturing *Nannochloropsis oculata*

Substances	Composition (g/l of water)
KNO_3	100
NaH_2PO_4	10
Na_2EDTA	10
$FeCl_3$	1.3

Chemical composition

Energy-dispersive X-ray (EDX) spectrometry was used to determine the chemical composition of algal biomass. Scanning electron microscope images were taken by FEI Inspect S50 equipped with X-ray microanalysis capabilities (AMETEK EDAX^{TSL}). Samples were gold coated to minimize the effect of electron charging of the surface, which could distort the images.

Lipid extraction

The total lipid of *N. oculata* was extracted using a Soxhlet extractor system. Approximately 3 g of biomass powder was weighed into a cellulose thimble inside the extraction chamber. A total of 150 ml pure *n*-hexane was used to extract the lipid for 6 h at the rate of 10 refluxes per hour to achieve maximum extraction efficiency. The extracted lipid was measured after removing the solvent using vacuum rotary evaporator to evaporate the *n*-hexane at 35 °C for 60 min, and then lipid content was calculated. The adopted Soxhlet unit description could be found in different literature [37].

Proximate analysis

The moisture, volatile matter, fixed carbon, and ash content of the dry algal biomass were determined by thermal gravimetric analyzer (STA PT1600 by Linseis). The adopted method is basically described by Beamish [38] and Mayoral et al. [39]. Approximately 20 mg samples were loaded into an Al_2O_3 ceramic crucible. Initially, the sample was kept isothermally at 25 °C for 8 min. The heating ramp was set at 50 °C/min, from 25 °C up to 125 °C then held for 3 min. A new 80 °C/min heating ramp was programmed up to 950 °C and maintained at that temperature for a total duration of 40 min. The whole process was done using Argon as purge gas to guarantee a non-oxidative environment. However, this gas was then switched to the air atmosphere when it was achieved isothermally at 40 min. Once a constant mass loss was reached, the isothermally final temperature was maintained for a total duration of 65 min in the air atmosphere to complete the combustion process. The moisture, volatile matter, fixed carbon, and ash were calculated by the difference from slope to slope of thermogravimetric (TG) curve.

Determination of higher heating value (HHV)

The heating value of microalgal biomass was evaluated by an equation proposed by Nhuchhen and Abdul Salam [40]. This calculation was based on values resulted from the proximate analysis.

$$\mathrm{HHV} = 19.2880 - 0.2135 \cdot \mathrm{VM/FC} + 0.0234 \cdot \mathrm{FC}/A - 1.9584 \cdot A/\mathrm{VM} \quad (3)$$

where, VM, FC, and A were volatile matter, fixed carbon, and ash content of biomass, respectively, by dry weight basis.

FTIR analysis

The infrared spectrum of dried algal biomass and its residue were recorded by Shimadzu FTIR spectroscopy. Both kinds of samples were mixed with potassium bromide (KBr) powder, and then pressed into tablets before measurement. Samples were scanned from 400 to 4,000/cm.

Results and discussion

One of microalgae potential's benchmarks as biomass fuel feedstock is determined by the abundance of the biomass so the availability will be assured. Therefore, the biomass productivity of algae in terms of growth rate is one of the most significant parameters that must be examined.

The biomass yields of *N. oculata* during 7-day cultivation period were depicted in Fig. 1. These results showed that *N. oculata* multiplied its biomass rapidly, starting at around 2×10^6 cells/ml on day 1 to approximately 12×10^6 cells/ml on day 7. It meant the average increase in biomass was approximately 1.5×10^6 cells/ml/day, higher than that of *Selenastrum* sp., which increase in cell number per day was about 1.6×10^4 up to 2.2×10^4 cells/ml/day [41]. If the productivity of *N. oculata* was expressed in growth kinetics, then it had specific growth rate of 0.27/day and doubling time of 2.59 days as shown in Table 2. Its growth kinetics revealed that *N. oculata* biomass productivity was higher than *Dunaliella salina* [42], *S. obliquus* [43], and *C. vulgaris* [44], which their growth rates were 0.18, 0.22, and 0.14/day, and their doubling time were 3.85, 3.15, and 4.95 days, respectively. This result was important to note by considering the *N. oculata* had been cultivated in the traditionally natural open pond as illustrated in Fig. 2a. The products of biomass sediment, the dried biomass chunk and the biomass powder of *N. oculata*, were shown at Fig. 2b–d, respectively. By fitting the curve of Fig. 1, the growth pattern of *N. oculata* could be estimated as an order 3 of a polynomial equation as $Y = 2{,}018{,}570 - 736{,}666.67X + 783{,}095.24X^2 - 66{,}666.67X^3$ with the fitting degree (R^2) of 0.999, where Y and X were cell density and cultivation time, respectively.

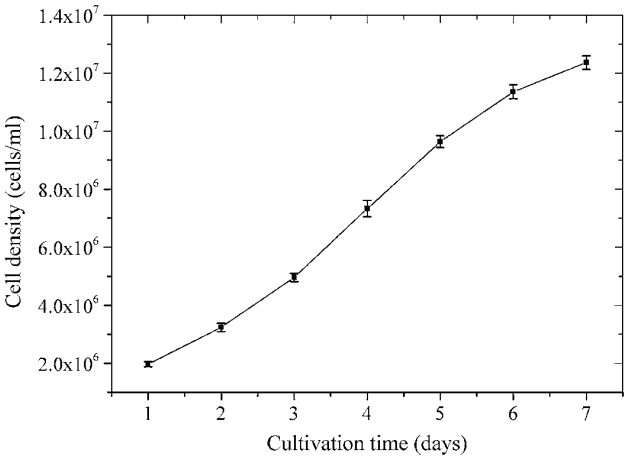

Fig. 1 The cell density of *Nannochloropsis oculata* during 7-day cultivation period. Relative standard error of means were below 5 % for all situations

The properties of algal biomass as a biofuel source were taken into consideration in this study. These properties varied widely, depended on the kind of algae, environmental culturing, cultivation periods, and harvesting conditions. Hence, investigating these properties was essential to determine the proper combustion technology.

Figure 3 showed the EDX spectrograms of *N. oculata* biomass for determination of its compositions as compiled in Table 2. Generally, the investigated *N. oculata* biomass has low carbon, high oxygen, and high inorganic elements compared to the result of Patil et al. [45]. These compositions had an impact on biomass combustion and the residual characteristics. They were also needed for

Table 2 The growth kinetics parameters and properties of *Nannochloropsis oculata*

Parameters/properties	Values
Specific growth rate (/day)	0.27
Doubling time (day)	2.59
Lipid content (%)	11.44
EDX analysis (wt%)	
C	28.32
O	43.80
Na	2.04
Mg	13.16
Al	0.92
Si	1.60
Cl	1.97
Ca	8.20
Proximate analysis (wt%)	
M (adb)	3.99
VM (db)	67.45
FC (db)	8.08
A (db)	24.47
HHV analysis (MJ/kg)	16.80

adb air-dried basis, *db* dry basis

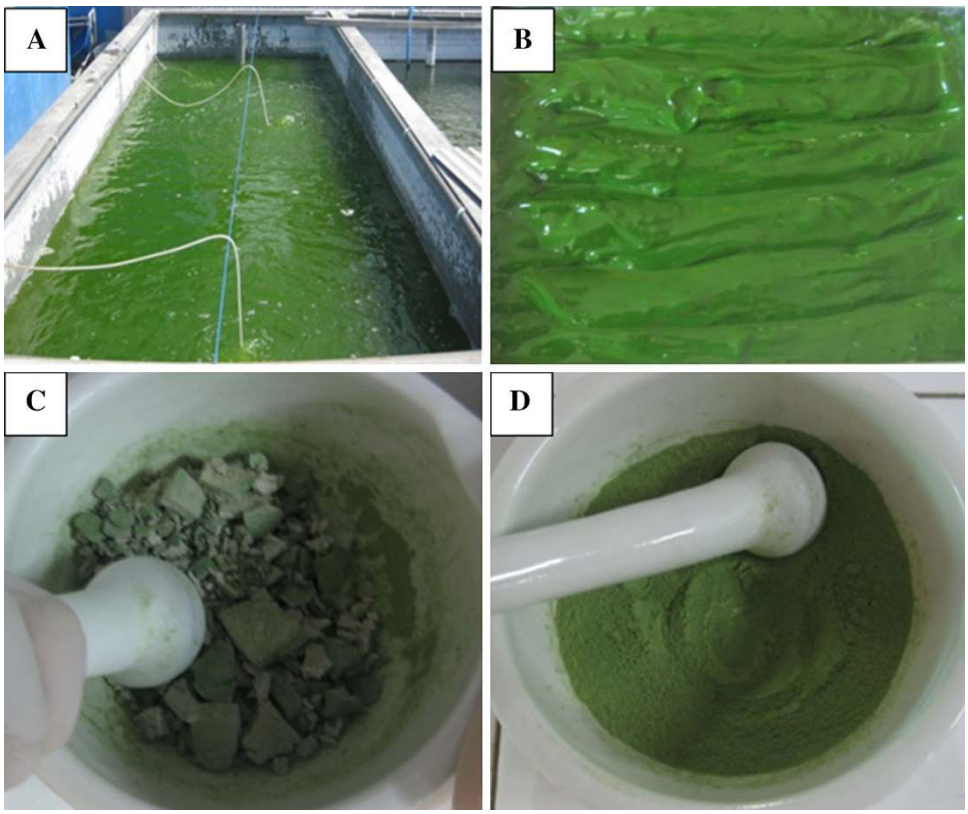

Fig. 2 The cultivation pond (**a**), the biomass sediment (**b**), the dried biomass chunk (**c**), and biomass powder (**d**) of *Nannochloropsis oculata*

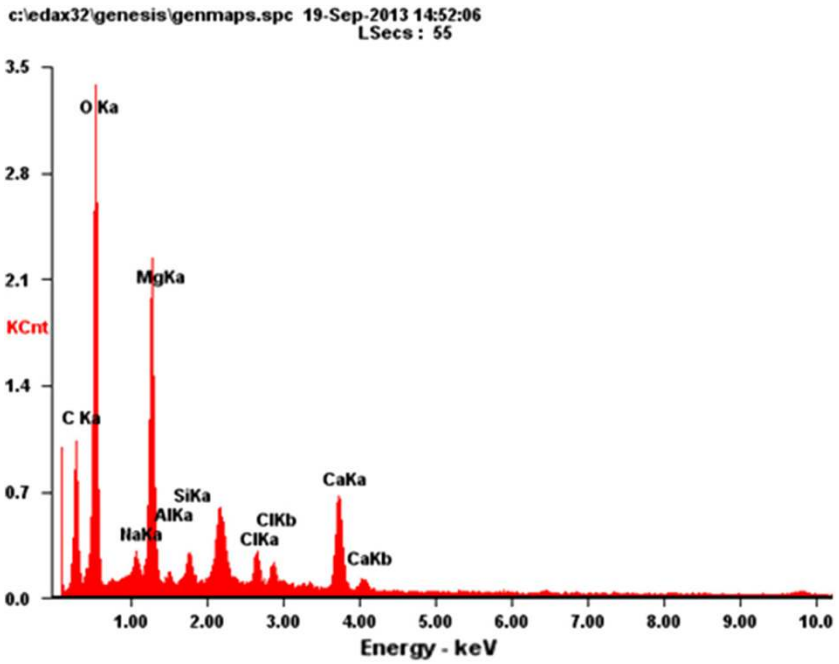

Fig. 3 EDX spectrograms of *Nannochloropsis oculata* biomass

estimating the air required for the combustion process and for predicting the released gases. Carbon was oxidized during combustion by exothermic reactions and formed CO_2. The organically bound of oxygen is released as the result of thermal processes, and it supplies a part of the overall oxygen needed for the combustion reactions [14].

The high amount presence of inorganic materials in this biomass, especially magnesium, calcium, sodium, silicon, and chlorine needs to be considered because they

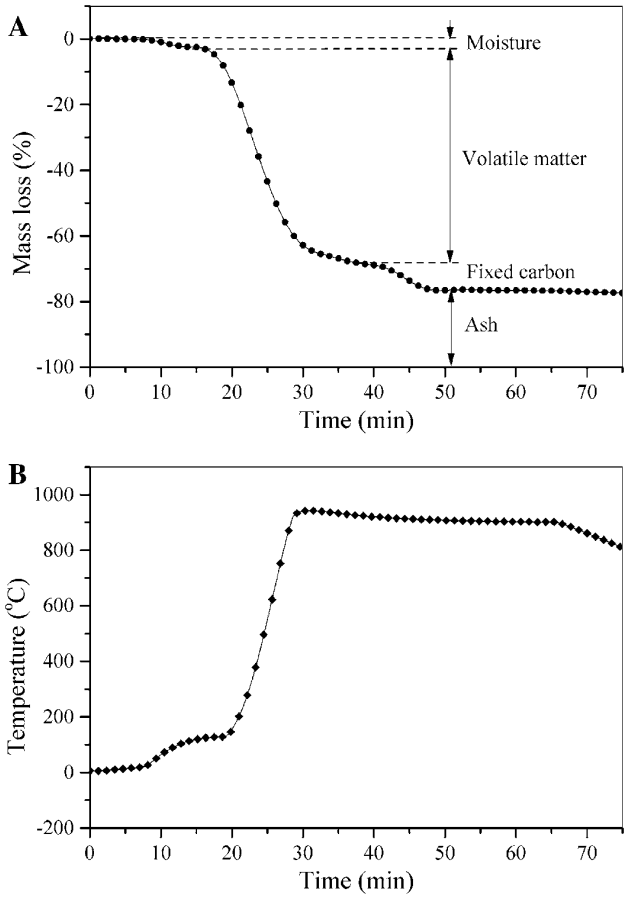

Fig. 4 TG curve for determining the proximate value. **a** Mass loss (%) vs. time (min) and **b** temperature setting (°C) vs. time (min)

frequently results in slagging and fouling problems in furnaces. The reaction of alkali metals with silica presented in the ash can lead to the formation of low-melting silicates in fly ash particles yielding a sticky, mobile liquid phase, which causes blockages of airways in the furnace and boiler plant [46]. Cl vaporized during combustion, forming HCl, Cl_2, and alkali chlorides. Alkali and alkaline earth chlorides are condensed in the boiler section as fly- ash particles or on the heat exchanger surfaces when flue gas temperature decreases [47]. Parts of the Cl were bounded in the fly ash while the rests were emitted as HCl in the flue gas. HCl emissions could play in the corrosion of metal component plant such as boilers and air pollution control devices.

The TG curve for determining the proximate value was shown in Fig. 4. The values of moisture (*M*), volatile matter (VM), fixed carbon (FC), and ash (*A*) were directly determined from the TG curve by the difference while higher heating value (HHV) of the biomass was estimated by Eq. (3). All of these results were tabulated in Table 2.

As shown in Fig. 4, the first mass loss, which was indicated by the reaching of the first constant mass line, corresponded to moisture loss. The *N. oculata* moisture content was 3.99 %, which seemed to be a potential candidate for direct combustion. The moisture content influenced the combustion behavior and the amount of energy to evaporate water. The water content in the fuel had to be released before the first step combustion starting; hence high moisture content of biomass meant more energy for evaporation, and subsequently for heating the water vapor. Removal of water in the biomass would decrease the maximum possible combustion temperature and overall system efficiency. Aside from moisture evaporation that consumed a great deal of heat, it also caused the evaporation time to be extended during the combustion process. Hence, it resulted in the decay of ignition and affected the necessary residence time of biomass fuel in the combustion chamber before gasification and combustion taking place. Consequently, the high moisture fuel contents would require the larger combustion chambers and would result in an expansive boiler. Moreover, the amount of moisture also affected the burning reaction rate; thus, it influenced the generated gas emission as NO and CO, as well. In the devolatilization process, due to evaporated moisture moves away from the devolatilization front, the amount of volatile determined the reaction zone thickness [48], and it influenced the heat transfer to the devolatilization zone which affected the devolatilization rate. Thus, the moisture content was very important fuel parameter, and investigating this parameter was required to adjust the temperature control system of the furnace properly.

In line with the rising temperature, a major part of biomass organic component experienced thermal cracking then decomposed and volatilized to be the volatile matter. In inert gas, the volatile is released at temperature up to 900 °C [39]. For microalgal biomass, it was especially resulted from the thermal cleavage of proteins, carbohydrates, and lipids. Table 2 showed that *N. oculata* volatile matter content was 67.45 %, lower than *Chlorella* sp. MP-1 that was 77.45 % [49] and higher than *C. vulgaris* that was 55.37 % [50]. The amount of biomass volatile matter strongly influenced the thermal decomposition and the combustion behavior. As it had been previously stated that the biomass, which had a high amount of volatiles, would be degraded as a result of the heating process. A significant part of the biomass was vaporized earlier before homogeneous gas phase combustion reactions took place and subsequently the remaining char undergone heterogeneous combustion reactions. Because of volatile matter was the reactive substance, hence, more volatile meant easier biomass to be burned. The aforementioned phenomenon would determine both of the ignition and burnout time of volatiles in the first stage of combustion processes, as well as the char combustion in the second stage. Moreover, in the context of co-combustion with other solid fuel, higher

volatile could create larger fuel-rich regions in the near-burner region. The fuel-rich regions were very critical area. They were used for flame stabilization but, the formation of undesired prompt NO_x, H_2S, and soot could occur in this zone, as well [51–53]. Hence, finding out its amount is necessary to adjust the sufficiency of air supplied in the zone where volatile is released to improve combustion efficiency. Furthermore, the appropriate composition of supplied air in the released volatile zone will affect the formation of soot and NO emissions as discussed earlier by Liu et al. [54, 55].

The fixed carbon content, which was the mass left over after the releases of volatiles excluding the ash and moisture contents, produced a char and was burned as a solid material in the combustion system. The *N. oculata* fixed carbon content was 8.08 %. This content was lower than both of *C. vulgaris* [50] and *Chlorella* sp. MP-1 [49], which were 34.35 and 16.95 %, respectively. The volatile matter and fixed carbon contents significance were that they provided a measure of the ease which the biomass could be gasified and oxidized in the combustion process. The *N. oculata* biomass, which had high volatile matter and low fixed carbon contents, was highly reactive fuel and would give a faster combustion rate during the devolatilization phase. This amount of fixed carbon was also needed to estimate the heating value of biomass, and it was acted as the main heat generator during the burning process.

The final residual material after the combustion process of biomass was ash, and it formed a standard measurement parameter for solid fuels. Table 2 indicated that *N. oculata* ash content was 24.47 %, which was very high, four times higher than *Chlorella* sp. MP-1 that was 6.36 % [49]. It was in accordance with the EDX analysis results, which showed the inorganic components content of *N. oculata* was high, as well. Inorganic components in biomass had a direct influence in the ash formation. Ash-forming elements exist in biomass as salts [14], bounded in the carbon structure, or they present as mineral particles from cultivation environment and introduce into the biomass fuel during harvest. In the combustion process, the part of the ash-forming compounds in biomass was vaporized and released to the gas phase while non-vaporized ash compounds that were left over in the char might melt and coalesce inside and on the surface of the char. The vaporized compounds would either be condensed or reacted on the surface of pre-existing ash particles in the flue gas when its temperature decreased. All of these could contribute to bed agglomeration, heat transfer surface fouling, and system corrosion. Furthermore, in the combustion process, the ash resulted from char burning would be formed as the layer surrounding their surface; hence, it inhibited the oxygen diffusion during char combustion. It affects both burning rate and mass loss rate, as well [56]. To address the problem of *N. oculata*'s high ash content during thermal conversion processes, it might suitably blend this biomass in terms of co-combustion with other feedstocks to obtain the overall low ash content. One of the low ash biomass was rice straw, which its ash content was around 0.1–0.7 % by dry weight [57]. It might appropriate be blended with *N. oculata* to be mixed biomass fuel feedstock. However, their characteristics have not been studied yet.

Higher heating value was a total of heat yielded by the complete combustion of a unit quantity of fuels, including the latent heat contained in the water vapor. Therefore, it represented the maximum amount of energy which was

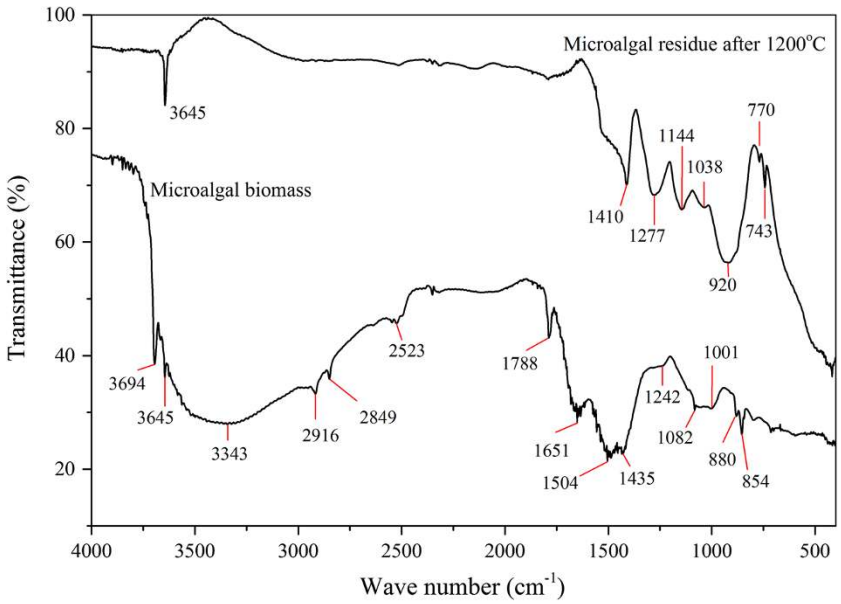

Fig. 5 FTIR spectra of *Nannochloropsis oculata* biomass and its residue

Table 3 Tentative assignments of bands found in the FTIR spectra of *Nannochloropsis oculata* biomass

Band	Main peak (/cm)	Wave number range (/cm)	Typical band assignment	References
1	3,694	3,759–3,676	Water ν(O–H) stretching of silanol and adsorbed water	[62, 63]
2	3,645	3,659–3,636	Water ν(O–H) stretching of silanol and adsorbed water Protein ν(N–H) stretching (amide A)	[62, 64, 65]
3	3,343	3,512–3,003	Water ν(O–H) stretching Protein ν(N–H) stretching (amide A)	[64–68]
4	2,916	2,940–2,897	Lipid $\nu_{as}(CH_2)$ stretching of methylene	[49, 64, 69]
5	2,849	2,860–2,835	Lipid $\nu_{s}(CH_2)$ stretching of methylene	[49, 64, 68–70]
6	2,523	2,571–2,509	Protein Superimposed (O–H) and $-NH_3^+$ stretching	[63]
7	1,788	1,811–1,765	Lipid (fatty acids) Protein ν(C=O) stretching of esters	[49, 66, 68, 69, 71–74]
8	1,651	1,692–1,599	Protein Amide I band mainly ν(C=O) stretching	[49, 64, 66–69, 71, 74–80]
9	1,504	1,545–1,460	Protein Amide II band mainly ν(C–H) and δ(N–H) associate with proteins DNA (cytosine) In-plane double bond base vibrations, which include C=C, C=N and C=O stretching	[64, 65, 67–69, 71, 74–76, 80–83]
10	1,435	1,445–1,416	DNA (Adenine) Protein $\delta_{as}(CH_2)$ and $\delta_{as}(CH_3)$ bending of methyl Carboxylic group ν(C–O) stretching	[64, 66, 67, 69, 74, 75, 80, 82]
11	1,242	1,312–1,204	DNA-phospholipids Phosphodiester of nucleic acids and phospholipid Antisymmetric PO_2^- stretching (ν_{as} P=O)	[64–68, 73, 75, 79, 80, 82, 83]
12	1,082	1,101–1,070	Phospholipids, DNA and RNA ν_{s}(P=O) Carbohydrates ν(C–O) stretching ν(C–O–C) stretching of polysaccharides Siloxane, silicate frustules ν(Si–O)	[62, 64–69, 71, 73–75, 80–86]
13	1,001	1,020–957	Siloxanes ν(Si–O) Silanes Si–OH bond stretching Carbohydrates ν(C–O) stretching ν(C–O–C) stretching of polysaccharides RNA–DNA Ribose ν_{as}(P=O)	[62, 67–69, 74, 75, 79–82, 84–86]
14	880	893–870	Polysaccharides of the cell wall β-D-glucans deformation δ(C–H) Silanol δ(Si–OH) bending	[62, 69, 70, 78, 83, 84, 87–91]
15	854	866–839	Polysaccharides of the cell wall α-D-glucans deformation δ(C–H) aromatic deformation Silanol δ(Si–OH) bending	[62, 70, 88, 92–96]

ν stretching, δ deformation, *subscript s* symmetric, *subscript as* asymmetric

potentially recoverable from a given biomass source. Based on the proximate result, HHV of *N. oculata* was 16.80 MJ/kg. This value was lower than both of *C. vulgaris* and *C. minutissima* that were 18 and 21 MJ/kg, respectively [9]. According to Illman et al. [9] the heating value of algae is in correlation with the lipid content of their biomass rather than with other components such as carbohydrates and proteins. As a comparison, the lipid content of *N. oculata* in this work was about 11 %, whereas *C. vulgaris* and *C. minutissima* lipid content were 18 and 31 %, respectively [9].

The FTIR spectrum of *N. oculata* biomass and its residue were shown in Fig. 5. For the biomass, it could be observed fifteen distinct transmission bands over the wave number range of 4,000–400/cm. These bands were assigned to specific molecular groups and were tentatively identified on the basis of biochemical reference standards and published FTIR spectra as quoted in Table 3. The cellular macromolecules (proteins, lipids, and carbohydrates) could be identified by their distinct transmittance in different frequency regions. The "carbohydrate band spectra" was characterized by weak and medium features at around 1,101–839/cm due to C–O and C–O–C stretching, Si–O stretching of siloxane silicate frustules, Si–OH bond stretching and bending of silanol. The "protein band spectra" was presented as less pronounced band at about 1,242/cm owing to asymmetric stretching of phosphodiester P=O. The spectrum of 1,435/cm related to CH_2 and CH_3 bending of methyl and C–O stretching of carboxylic group. The band at around 1,504/cm was amide II band spectra mainly ν(C–H) and δ(N–H). The medium amide I band at around 1,811–1,599/cm was primarily for C=O stretching of esters. The less pronounced band at 2,523/cm and around 3,659–3,003/cm because of amine salts $-NH_3^+$ stretching and N–H stretching of amide A, respectively. The bands associated with "lipid band spectra" were indicated by two weak peaks at around 2,940–2,835/cm related to CH_2 stretching of methylene and a strong peak at 1,788/cm as a result of C=O stretching of esters. The aforementioned bands spectra have specified the presence of the principal components in the *N. oculata*, namely carbohydrate, protein, and lipid. These components derived from various microalgae cell structure, such as a cell wall, plasma membrane, chloroplasts, mitochondrion, etc. Each cell structure substance would be progressively destroyed during the thermal processes when the temperature reached its decomposition temperature, and part of it released and formed volatile matter, whereas the remaining substance formed char as a solid material. Both of volatile and char would be burned through the combustion processes. The last rests after their complete burning processes were ash as residual materials.

Microalgal residue bands spectra were characterized by a strong feature at 3,645/cm related to O–H stretching of adsorbed water by silica presented in the ash, and strong, medium, and weak features at the fingerprint area associated with the rest of the inorganic component which was left in the ash. The band spectra between 1,490 and 1,410/cm correlated with calcium carbonate, mainly due to antisymmetric CO_3– stretching [58]. The features at around 1,200–900/cm region associated with the silica structure, especially due to Si–O stretching modes [59]. The peaks below 800/cm were vibrations of Ca–O and Mg–O [60]. The strong band at around 400–500/cm is caused by Si–O or Al–O bending vibrations [61]. The elements of ash content were critical parameter in that case of byproduct handling and utilization, as well as they have an impact on the overall processing cost of biomass conversion. However, the ash characterization, other than FTIR that have been previously stated, was not performed in this research, and it will be extensively investigated in the future studies.

Figure 5 revealed the progressive degradation intensity in the spectra of biomass residue after 1,200 °C, mainly at around 3,590–1,630/cm. The declined intensity was caused by the loss of protein and lipid components of biomass during thermal processes. The feature changes at fingerprint area associated with protein degradation of biomass mainly amide II. It also correlated with degradation of cell wall structures including their fibrillar component that composed of polymer of β-D-glucose and their amorphous mucilaginous material which constituted polysaccharides, lipids, and proteins.

Conclusions

The potential and properties of *N. oculata* biomass for futuristic renewable fuel have been studied. With traditionally natural and low-cost nutrient cultivation, this algae species grows rapidly. The physicochemical properties of this biomass also indicated that it is feasible as biofuel feedstock, except for its high content of inorganic components, which need special attention. The aforementioned attributes allow *N. oculata* to be a strong alternative renewable fuel, either by direct combustion under the proper handling for its residue or by co-combustion with other biomass feedstocks, which have low ash content such as rice straw, for reducing ash product. To optimize the usefulness of this biomass related to its productivity and appropriateness of combustion technology, it requires further in-depth research.

Authors' contributions Sukarni drafted the manuscript. All authors read and approved the final manuscript.

Acknowledgments This work was supported by Directorate General of Higher Education, the Ministry of Education and Culture, Republic of Indonesia; the Fundamental Research Funds, in accordance with the Agreement on Implementation and Assignment Research Program Number 023.04.1.673,453/2012, December 5, 2012, the second revision in May 1, 2013. The authors would like to thank Mrs. Wiwie, Mr. Praptono, and Mr. Sugeng Joko Purnomo from the Institute of Brackish Water Aquaculture (BBAP) Situbondo for facilitating the microalgae cultivation.

Conflict of interest The authors declare that they have no competing interests.

References

1. Yaman, S.: Pyrolysis of biomass to produce fuels and chemical feedstocks. Energy Convers. Manag. **45**(5), 651–671 (2004)
2. Özçimen, D., Karaosmanoğlu, F.: Production and characterization of bio-oil and biochar from rapeseed cake. Renew. Energy **29**(5), 779–787 (2004)
3. Brennan, L., Owende, P.: Biofuels from microalgae—a review of technologies for production, processing, and extractions of biofuels and co-products. Renew. Sustain. Energy Rev. **14**(2), 557–577 (2010)
4. Tabatabaei, M., Tohidfar, M., Jouzani, G.S., Safarnejad, M., Pazouki, M.: Biodiesel production from genetically engineered microalgae: future of bioenergy in Iran. Renew. Sustain. Energy Rev. **15**(4), 1918–1927 (2011)
5. Gonçalves, A., Pires, J., Simões, M.: Lipid production of *Chlorella vulgaris* and *Pseudokirchneriella subcapitata*. Int. J. Energy Environ. Eng. **4**(1), 1–6 (2013)
6. Li, Y., Horsman, M., Wu, N., Lan, C.Q., Dubois-Calero, N.: Biofuels from microalgae. Biotechnol. Prog. **24**(4), 815–820 (2008)
7. Hu, Q., Sommerfeld, M., Jarvis, E., Ghirardi, M., Posewitz, M., Seibert, M., et al.: Microalgal triacylglycerols as feedstocks for biofuel production: perspectives and advances. Plant J. **54**(4), 621–639 (2008)
8. Chisti, Y.: Biodiesel from microalgae. Biotechnol. Adv. **25**(3), 294–306 (2007)
9. Illman, A., Scragg, A., Shales, S.: Increase in chlorella strains calorific values when grown in low nitrogen medium. Enzyme Microb. Technol. **27**(8), 631–635 (2000)
10. Gouveia, L., Marques, A.E., da Silva, T.L., Reis, A.: Neochloris oleabundans utex #1185: a suitable renewable lipid source for biofuel production. J. Ind. Microbiol. Biotechnol. **36**(6), 821–826 (2009)
11. Mandotra, S.K., Kumar, P., Suseela, M.R., Ramteke, P.W.: Fresh water green microalga *Scenedesmus abundans*: a potential feedstock for high quality biodiesel production. Bioresour. Technol. **156**, 42–47 (2014)
12. Schenk, P.M., Thomas-Hall, S.R., Stephens, E., Marx, U.C., Mussgnug, J.H., Posten, C., et al.: Second generation biofuels: high-efficiency microalgae for biodiesel production. Bioenergy Res. **1**(1), 20–43 (2008)
13. Akowuah, J.O., Kemausuor, F., Mitchual, S.J.: Physico-chemical characteristics and market potential of sawdust charcoal briquette. Int. J. Energy Environ. Eng. **3**(1), 1–6 (2012)
14. Van Loo, S., Koppejan, J.: The Handbook of Biomass Combustion and Co-firing. Earthscan, London (2008)
15. Raveendran, K., Ganesh, A., Khilar, K.: Influence of mineral matter on biomass pyrolysis characteristics. Fuel **74**(12), 1812–1822 (1995)
16. Xiao, R., Chen, X., Wang, F., Yu, G.: The physicochemical properties of different biomass ashes at different ashing temperature. Renew. Energy **36**(1), 244–249 (2011)
17. Doshi, V., Vuthaluru, H.B., Korbee, R., Kiel, J.H.A.: Development of a modeling approach to predict ash formation during cofiring of coal and biomass. Fuel Process. Technol. **90**(9), 1148–1156 (2009)
18. Wei, X., Schnell, U., Hein, K.: Behaviour of gaseous chlorine and alkali metals during biomass thermal utilisation. Fuel **84**(7–8), 841–848 (2005)
19. Du, S., Yang, H., Qian, K., Wang, X., Chen, H.: Fusion and transformation properties of the inorganic components in biomass ash. Fuel **117**, 1281–1287 (2014)
20. Obernberger, I., Brunner, T., Barnthaler, G.: Chemical properties of solid biofuels—significance and impact. Biomass Bioenergy **30**(11), 973–982 (2006)
21. Hibberd, D.J.: Notes on the taxonomy and nomenclature of the algal classes eustigmatophyceae and tribophyceae (synonym xanthophyceae). Bot. J. Linn. Soc. **82**(2), 93–119 (1981)
22. Karlson, B., Potter, D., Kuylenstierna, M., Andersen, R.A.: Ultrastructure, pigment composition, and 18 s rrna gene sequence for *Nannochloropsis granulata* sp. nov. (monodopsidaceae, eustigmatophyceae), a marine ultraplankter isolated from the Skagerrak, northeast atlantic ocean. Phycologia **35**(3), 253–260 (1996)
23. Gwo, J.-C., Chiu, J.-Y., Chou, C–.C., Cheng, H.-Y.: Cryopreservation of a marine microalga, *Nannochloropsis oculata* (eustigmatophyceae). Cryobiology **50**(3), 338–343 (2005)
24. Hu, H., Gao, K.: Optimization of growth and fatty acid composition of a unicellular marine picoplankton, Nannochloropsis sp., with enriched carbon sources. Biotechnol. Lett. **25**(5), 421–425 (2003)
25. Whittle, S.J., Casselton, P.J.: The chloroplast pigments of the algal classes eustigmatophyceae and xanthophyceae. I. Eustigmatophyceae. Br. Phycol. J. **10**(2), 179–191 (1975)
26. Volkman, J.K., Brown, M.R., Dunstan, G.A., Jeffrey, S.: The biochemical composition of marine microalgae from the class eustigmatophyceae. J. Phycol. **29**(1), 69–78 (1993)
27. Adl, S.M., Simpson, A.G.B., Farmer, M.A., Andersen, R.A., Anderson, O.R., et al.: The new higher level classification of eukaryotes with emphasis on the taxonomy of protists. J. Eukaryot. Microbiol. **52**(5), 399–451 (2005)
28. Barsanti, L., Gualtieri, P.: Algae: Anatomy, Biochemistry, and Biotechnology. CRC Press, Boca Raton (2006)
29. Fogg, G.E.: Some comments on picoplankton and its importance in the pelagic ecosystem. Aquat. Microb. Ecol. **9**, 33–39 (1995)
30. Lubián, L.M., Montero, O., Moreno-Garrido, I., Huertas, I.E., Sobrino, C., González-del Valle, M., et al.: Nannochloropsis (eustigmatophyceae) as source of commercially valuable pigments. J. Appl. Phycol. **12**(3), 249–255 (2000)
31. Lee, M.-Y., Min, B.-S., Chang, C.-S., Jin, E.: Isolation and characterization of a xanthophyll aberrant mutant of the green alga *Nannochloropsis oculata*. Mar. Biotechnol. **8**(3), 238–245 (2006)
32. Osinga, R., Kleijn, R., Groenendijk, E., Niesink, P., Tramper, J., Wijffels, R.H.: Development of in vivo sponge cultures: particle feeding by the tropical sponge Pseudosuberites aff. andrewsi. Mar. Biotechnol. New York NY **3**(6), 544–554 (2001)
33. Ferreira, M., Coutinho, P., Seixas, P., Fábregas, J., Otero, A.: Enriching rotifers with "premium" microalgae. *Nannochloropsis gaditana*. Mar. Biotechnol. **11**(5), 585–595 (2009)

34. Rodolfi, L., Chini Zittelli, G., Bassi, N., Padovani, G., Biondi, N., Bonini, G., et al.: Microalgae for oil: strain selection, induction of lipid synthesis and outdoor mass cultivation in a low-cost photobioreactor. Biotechnol. Bioeng. **102**(1), 100–112 (2009)
35. Griffiths, M.J., Harrison, S.T.L.: Lipid productivity as a key characteristic for choosing algal species for biodiesel production. J. Appl. Phycol. **21**(5), 493–507 (2009)
36. Andersen, R.A. (ed.): Algal Culturing Techniques. Elsevier Academic Press, London (2005)
37. Wang, L., Weller, C.L.: Recent advances in extraction of nutraceuticals from plants. Trends Food Sci. Technol. **17**(6), 300–312 (2006)
38. Beamish, B.B.: Proximate analysis of New Zealand and Australian coals by thermogravimetry. New Zeal. J. Geol. Geophys. **37**(4), 387–392 (1994)
39. Mayoral, M.C., Izquierdo, M.T., Andres, J.M., Rubio, B.: Different approaches to proximate analysis by thermogravimetry analysis. Thermochim. Acta **370**, 91–97 (2001)
40. Nhuchhen, D.R., Abdul Salam, P.: Estimation of higher heating value of biomass from proximate analysis: a new approach. Fuel **99**, 55–63 (2012)
41. Goswami, R., Kalita, N., Kalita, M.C.: A study on growth and carbon dioxide mitigation by microalgae *Selenastrum* sp.: its growth behavior under different nutrient environments and lipid production. Ann. Biol. Res. **3**(1), 499–510 (2012)
42. García-González, M., Moreno, J., Manzano, J.C., Florencio, F.J., Guerrero, M.G.: Production of *Dunaliella salina* biomass rich in 9-*cis*-beta-carotene and lutein in a closed tubular photobioreactor. J. Biotechnol. **115**(1), 81–90 (2005)
43. De Morais, M.G., Costa, J.A.V.: Biofixation of carbon dioxide by *Spirulina* sp. and *Scenedesmus obliquus* cultivated in a three-stage serial tubular photobioreactor. J. Biotechnol. **129**(3), 439–445 (2007)
44. Converti, A., Casazza, A.A., Ortiz, E.Y., Perego, P., Del Borghi, M.: Effect of temperature and nitrogen concentration on the growth and lipid content of *Nannochloropsis oculata* and *Chlorella vulgaris* for biodiesel production. Chem. Eng. Process. Process Intensif. **48**(6), 1146–1151 (2009)
45. Patil, P.D., Gude, V.G., Mannarswamy, A., Cooke, P., Munson-McGee, S., Nirmalakhandan, N., et al.: Optimization of microwave-assisted transesterification of dry algal biomass using response surface methodology. Bioresour. Technol. **102**(2), 1399–1405 (2011)
46. McKendry, P.: Energy production from biomass (part 1): overview of biomass. Bioresour. Technol. **83**(1), 37–46 (2002)
47. Biedermann, F., Obernberger, I.: Ash-related problems during biomass combustion and possibilities for a sustainable ash utilisation. In: Proceedings of Int. Conf. 'World Renew. Energy Congr. Elsevier Ltd, Aberdeen (2005)
48. Yang, Y.B., Sharifi, V.N., Swithenbank, J.: Effect of air flow rate and fuel moisture on the burning behaviours of biomass and simulated municipal solid wastes in packed beds. Fuel **83**(11–12), 1553–1562 (2004)
49. Phukan, M.M., Chutia, R.S., Konwar, B.K., Kataki, R.: Microalgae chlorella as a potential bio-energy feedstock. Appl. Energy **88**, 3307–3312 (2011)
50. Chen, C., Ma, X., Liu, K.: Thermogravimetric analysis of microalgae combustion under different oxygen supply concentrations. Appl. Energy **88**(9), 3189–3196 (2011)
51. Wiinikka, H.: High Temperature Aerosol Formation and Emission Minimisation during Combustion of Wood Pellets. Luleå University of Technology, Luleå (2005)
52. Hill, S., Douglas Smoot, L.: Modeling of nitrogen oxides formation and destruction in combustion systems. Prog. Energy Combust. Sci. **26**(4–6), 417–458 (2000)
53. Toftegaard, M.B., Brix, J., Jensen, P.A., Glarborg, P., Jensen, A.D.: Oxy-fuel combustion of solid fuels. Prog. Energy Combust. Sci. **36**(5), 581–625 (2010)
54. Liu, F., Guo, H., Smallwood, G.J., Gülder, Ö.L.: The chemical effects of carbon dioxide as an additive in an ethylene diffusion flame: implications for soot and NO_x formation. Combust. Flame **125**(1–2), 778–787 (2001)
55. Liu, J., Gao, S., Jiang, X., Shen, J., Zhang, H.: NO emission characteristics of superfine pulverized coal combustion in the O_2/CO_2 atmosphere. Energy Convers. Manag. **77**, 349–355 (2014)
56. Sukarni, Sudjito, Hamidi, N., Yanuhar, U., Wardana, I.N.G.: Thermogravimetric kinetic analysis of *Nannochloropsis oculata* combustion in air atmosphere. Front. Energy (2014) (accepted manuscript)
57. Liu, Z.: Energy from combustion of rice straw: status and challenges to china. Energy Power Eng. **03**(03), 325–331 (2011)
58. Bellamy, L.: The infra-red spectra of complex molecules. Chapman and Hall, London (1975)
59. Dodson, J.: Wheat straw ash and its use as a silica source. Dissertation, University of York (2011)
60. Abraham, R., George, J., Thomas, J., Yusuff, K.K.M.: Physicochemical characterization and possible applications of the waste biomass ash from oleoresin industries of India. Fuel **109**, 366–372 (2013)
61. Bai, J., Li, W., Li, B.: Characterization of low-temperature coal ash behaviors at high temperatures under reducing atmosphere. Fuel **87**(4–5), 583–591 (2008)
62. Parida, S.K., Dash, S., Patel, S., Mishra, B.K.: Adsorption of organic molecules on silica surface. Adv. Colloid Interface Sci. **121**(1–3), 77–110 (2006)
63. Silverstein, R.M., Webster, F.X., Kiemle, D.: Spectrometric Identification of Organic Compounds, 7th edn. Wiley, New Jersey (2005)
64. Sigee, D.C.D., Dean, A., Levado, E., Tobin, M.J.: Fourier-transform infrared spectroscopy of *Pediastrum duplex*: characterization of a micro-population isolated from a eutrophic lake. Eur. J. Phycol. **37**(1), 19–26 (2002)
65. Duygu, D.Y., Udoh, A.U., Ozer, T.B., Akbulut, A., Acikgoz, I., Yildiz, K., et al.: Fourier transform infrared (FTIR) spectroscopy for identification of *Chlorella vulgaris* Beijerinck 1890 and *Scenedesmus obliquus* (turpin) kützing 1833. Afr. J. Biotechnol. **11**(16), 3817–3824 (2012)
66. Murdock, J.N., Wetzel, D.L.: FT-IR microspectroscopy enhances biological and ecological analysis of algae. Appl. Spectrosc. Rev. **44**(4), 335–361 (2009)
67. Benning, L.G., Phoenix, V., Yee, N., Konhauser, K.: The dynamics of cyanobacterial silicification: an infrared micro-spectroscopic investigation. Geochim. Cosmochim. Acta **68**(4), 743–757 (2004)
68. Mayers, J.J., Flynn, K.J., Shields, R.J.: Rapid determination of bulk microalgal biochemical composition by Fourier-transform infrared spectroscopy. Bioresour. Technol. **148**, 215–220 (2013)
69. Jiang, Y., Yoshida, T., Quigg, A.: Photosynthetic performance, lipid production and biomass composition in response to nitrogen limitation in marine microalgae. Plant Physiol. Biochem. **54**, 70–77 (2012)
70. Marshall, C., Javaux, E., Knoll, A., Walter, M.: Combined micro-Fourier transform infrared (FTIR) spectroscopy and micro-Raman spectroscopy of proterozoic acritarchs: a new approach to palaeobiology. Precambrian Res. **138**(3–4), 208–224 (2005)
71. Gao, Y., Yang, M., Wang, C.: Nutrient deprivation enhances lipid content in marine microalgae. Bioresour. Technol. **147**, 484–491 (2013)
72. Tan, S.-T., Balasubramanian, R.K., Das, P., Obbard, J.P., Chew, W.: Application of mid-infrared chemical imaging and

multivariate chemometrics analyses to characterise a population of microalgae cells. Bioresour. Technol. **134**, 316–323 (2013)
73. Mecozzi, M., Pietroletti, M., Di Mento, R.: Application of FTIR spectroscopy in ecotoxicological studies supported by multivariate analysis and 2d correlation spectroscopy. Vib. Spectrosc. **44**(2), 228–235 (2007)
74. Stehfest, K., Toepel, J., Wilhelm, C.: The application of micro-FTIR spectroscopy to analyze nutrient stress-related changes in biomass composition of phytoplankton algae. Plant Physiol. Biochem. **43**(7), 717–726 (2005)
75. Benning, L.G., Phoenix, V., Yee, N., Tobin, M.: Molecular characterization of cyanobacterial silicification using synchrotron infrared micro-spectroscopy. Geochim. Cosmochim. Acta **68**(4), 729–741 (2004)
76. Ragusa, S., Cambria, M.T., Pierfederici, F., Scirè, A., Bertoli, E., Tanfani, F., et al.: Structure–activity relationship on fungal laccase from *Rigidoporus lignosus*: a Fourier-transform infrared spectroscopic study. Biochim. Biophys. Acta **1601**(2), 155–162 (2002)
77. Wysokowski, M., Behm, T., Born, R., Bazhenov, V.V., Meissner, H., Richter, G., et al.: Preparation of chitin-silica composites by in vitro silicification of two-dimensional *Ianthella basta* demosponge chitinous scaffolds under modified Stöber conditions. Mater. Sci. Eng. C. Mater. Biol. Appl. **33**(7), 3935–3941 (2013)
78. Kamnev, A., Ristić, M., Antonyuka, L.P., Chernyshev, A.V., Ignatov, V.V.: Fourier transform infrared spectroscopic study of intact cells of the nitrogen-fixing bacterium *Azospirillum brasilense*. J. Mol. Struct. **409**, 201–205 (1997)
79. Dean, A.P., Sigee, D.C., Estrada, B., Pittman, J.K.: Using FTIR spectroscopy for rapid determination of lipid accumulation in response to nitrogen limitation in freshwater microalgae. Bioresour. Technol. **101**(12), 4499–4507 (2010)
80. Dean, A.P., Nicholson, J.M., Sigee, D.C.: Impact of phosphorus quota and growth phase on carbon allocation in *Chlamydomonas reinhardtii*: an FTIR microspectroscopy study. Eur. J. Phycol. **43**(4), 345–354 (2008)
81. Meng, Y., Yao, C., Xue, S., Yang, H.: Application of Fourier transform infrared (FT-IR) spectroscopy in determination of microalgal compositions. Bioresour. Technol. **151**, 347–354 (2014)
82. Banyay, M., Sarkar, M., Gräslund, A.: A library of IR bands of nucleic acids in solution. Biophys. Chem. **104**, 477–488 (2003)
83. Jangir, D.K., Charak, S., Mehrotra, R., Kundu, S.: FTIR and circular dichroism spectroscopic study of interaction of 5-fluorouracil with DNA. J. Photochem. Photobiol. B **105**(2), 143–148 (2011)
84. Goo, B.G., Baek, G., Choi, D.J., Synytsya, A., Park, Y., Bleha, R., et al.: Characterization of a renewable extracellular polysaccharide from defatted microalgae *Dunaliella tertiolecta*. Bioresour. Technol. **129**, 343–350 (2013)
85. Guo, H., Daroch, M., Liu, L., Qiu, G., Geng, S., Wang, G.: Biochemical features and bioethanol production of microalgae from coastal waters of pearl river delta. Bioresour. Technol. **127**, 422–428 (2013)
86. El-Toni, A.M., Khan, A., Ibrahim, M.A., Labis, J.P., Badr, G., Al-Hoshan, M., et al.: Synthesis of double mesoporous core-shell silica spheres with tunable core porosity and their drug release and cancer cell apoptosis properties. J. Colloid Interface Sci. **378**(1), 83–92 (2012)
87. Lim, J.M., Joo, J.H., Kim, H.O., Kim, H.M., Kim, S.W., Hwang, H.J., et al.: Structural analysis and molecular characterization of exopolysaccharides produced by submerged mycelial culture of *Collybia maculata* tg-1. Carbohydr. Polym. **61**(3), 296–303 (2005)
88. Lecellier, A., Mounier, J., Gaydou, V., Castrec, L., Barbier, G., Ablain, W., et al.: Differentiation and identification of filamentous fungi by high-throughput FTIR spectroscopic analysis of mycelia. Int. J. Food Microbiol. **168–169**, 32–41 (2014)
89. Huang, G.L.: Extraction of two active polysaccharides from the yeast cell wall. Z. Naturforsch. C. **63**(11–12), 919–921 (2008)
90. Han, M., Han, J., Hyun, S., Shin, H.: Solubilization of water-insoluble beta-glucan isolated from Ganoderma lucidum. J. Environ. Biol. **29**(March), 237–242 (2008)
91. Jung, H.-K., Hong, J.-H., Park, S.-C., Park, B.-K., Nam, D.-H., Kim, S.-D.: Production and physicochemical characterization of β-glucan produced by *Paenibacillus polymyxa* jb115. Biotechnol. Bioprocess Eng. **12**, 713–719 (2007)
92. Peng, Y., Zhang, L., Zeng, F., Kennedy, J.F.: Structure and antitumor activities of the water-soluble polysaccharides from *Ganoderma tsugae* mycelium. Carbohydr. Polym. **59**(3), 385–392 (2005)
93. Huang, Q., Jin, Y., Zhang, L., Cheung, P.C.K., Kennedy, J.F.: Structure, molecular size and antitumor activities of polysaccharides from poria cocos mycelia produced in fermenter. Carbohydr. Polym. **70**(3), 324–333 (2007)
94. De Lourdes Corradida Silva, M., Fukuda, E.K., Vasconcelos, A.F.D., Dekker, R.F.H., Matias, A.C., Monteiro, N.K., et al.: Structural characterization of the cell wall D-glucans isolated from the mycelium of *Botryosphaeria rhodina* mamb-05. Carbohydr. Res. **343**(4), 793–798 (2008)
95. Tianqi, W., Hanxiang, L.I., Manyi, W., Tianwei, T.A.N.: Integrative extraction of ergosterol, (1 → 3)—α-D-glucan and chitosan from penicillium chrysogenum mycelia*. Chin. J. Chem. Eng. **15**(5), 725–729 (2007)
96. Peng, Y., Zhang, L., Zeng, F., Xu, Y.: Structure and antitumor activity of extracellular polysaccharides from mycelium. Carbohydr. Polym. **54**(3), 297–303 (2003)